Resonance enhanced Raman scatter in liquid benzene at vapor-phase absorption peaks

Adam Willitsford,[1] C. Todd Chadwick,[2] Hans Hallen,[2] Stewart Kurtz,[3] and C. Russell Philbrick[2,3,*]

[1] *Johns Hopkins University - Applied Physics Lab, Laurel, MD 20709 USA*
[2] *The North Carolina State University, Department of Physics, Raleigh, NC 27695 USA*
[3] *The Pennsylvania State University, Department of Electrical Engineering, University Park, PA 16802 USA*
[*] *philbrick@ncsu.edu*

Abstract: The resonance enhanced Raman spectra in the $^1B_{2u}$ mode of the forbidden benzene electronic transition band, ~230-270 nm, has been investigated. Resonance enhanced Raman scattering in both liquid benzene and liquid toluene exhibit the greatest enhancement when the wavelength of excitation is tuned to the vapor-phase absorption peaks; even though the sample volume is in a liquid state. Raman signals for the symmetric breathing mode of the carbon ring are found to be resonantly enhanced by several orders of magnitude (>500X) with deep UV excitation compared to non-resonant visible excitation. Since the benzene absorbs near this resonant wavelength, its effect on the sampled volume cannot be neglected in determining the resonance gain, as we discuss in detail. Large resonant gains correspond with excitation at the 247, 253, and 259 nm absorption peaks in the benzene vapor spectrum. The narrow region of resonance gain is investigated in detail around the absorption peak located at 259 nm using 0.25 nm steps in the excitation wavelength. We observe the resonance gain tracking the vapor phase absorption peaks and valleys within this narrow range. Results are interpreted in terms of the coherence forced by the use of a forbidden transition for resonance excitation.

OCIS codes: (260.5740) Resonance; (290.5860) Scattering, Raman; (040.7190) Ultraviolet; (300.1030) Absorption; (260.2510) Fluorescence; (300.0300) Spectroscopy.

References and links

1. L. Ziegler and B. Hudson, "Resonance Raman scattering of benzene and benzene-d_6 with 212.8 nm excitation," J. Chem. Phys. **74**(2), 982–992 (1981).
2. S. Asher and C. Johnson, "Resonance Raman excitation profile through the $^1B_{2u}$ state of benzene," J. Phys. Chem. **89**(8), 1375–1379 (1985).
3. D. Gerrity, L. Ziegler, P. Kelly, R. Desiderio, and B. Hudson, "Ultraviolet resonance Raman spectroscopy of benzene vapor with 220-184 nm excitation," J. Chem. Phys. **83**(7), 3209–3213 (1985).
4. R. Sension, R. Brudzynski, S. Li, B. Hudson, F. Zerbetto, and M. Z. Zgierski, "Resonance Raman spectroscopy of the B_{1u} region of benzene: analysis in terms of pseudo-Jahn-Teller Distortion," J. Chem. Phys. **96**(4), 2617–2628 (1992).
5. R. Sension, R. Brudzynski, and B. Hudson, "Vacuum ultraviolet resonance Raman studies of the valence electronic states of benzene and benzene-d_6: The E_{1u} state and a putative A_{2u} state," J. Chem. Phys. **94**(2), 873–882 (1991).
6. L. Ziegler and A. Albrecht, "Raman scattering of benzene in the ultraviolet," J. Chem. Phys. **67**(6), 2753–2757 (1977).
7. G. Korenowski, L. Ziegler, and A. Albrecht, "Calculations of resonance Raman cross sections in forbidden electronic transitions: scattering of the 992 cm^{-1} mode in the $^1B_{2u}$ band of benzene," J. Chem. Phys. **68**(3), 1248–1252 (1978).
8. A. Albrecht and M. Hutley, "On the dependence of vibrational Raman intensity on the wavelength of incident light," J. Chem. Phys. **55**(9), 4438–4443 (1971).
9. C. R. Philbrick, D. M. Brown, A. H. Willitsford, P. S. Edwards, A. M. Wyant, Z. Z. Liu, C. T. Chadwick, and H. Hallen, "Remote sensing of chemical species in the atmosphere," *Proc. 4th Lidar Atmos. Appl.* 89th AMS, 2009 *http://ams.confex.com/ams/pdfpapers/150051.pdf*

#196491 - $15.00 USD Received 27 Aug 2013; revised 6 Oct 2013; accepted 9 Oct 2013; published 24 Oct 2013

10. A. Sedlacek and C. Chen, "Exploitation of resonance Raman spectroscopy as a remote chemical sensor," *BNL-61359: Conf. 950787–35* (1995).
11. A. Sedlacek and C. Chen, "Remote detection of trace effluents using resonance Raman spectroscopy," *BNL-49542: Conf. 9311173–2* (1995).
12. C. Chen, D. Heglund, M. Ray, D. Harder, R. Dobert, K. Leung, M. Wu, and A. Sedlacek, "Application of resonance Raman lidar for chemical species identification," *BNL-64388: Conf.-970465–19* (1997).
13. C. L. Jahncke, H. D. Hallen, and M. A. Paesler, "Nano-Raman spectroscopy and imaging with the near-field scanning optical microscope," J. Raman Spectrosc. **27**(8), 579–586 (1996).
14. H. D. Hallen, "Nano-Raman spectroscopy: surface plasmon emission, field gradients, and fundamentally near field propagation effects," NanoBiotechnology **3**(3), 197 (2009), doi:10.1007/s12030-008-9013-1.
15. A. Willitsford, C. T. Chadwick, H. Hallen, and C. R. Philbrick, "Resonance Raman measurements utilizing a tunable deep UV source," Proc. SPIE **6950**, 695010 (2008).
16. A. Willitsford, *Resonance Raman Spectroscopy in the Ultraviolet using a Tunable Laser,* Ph.D. Dissertation, Penn State University (2008) *https://etda.libraries.psu.edu/paper/8149/*.
17. C. T. Chadwick, *Resonance Raman Spectroscopy Utilizing Tunable Deep Ultraviolet Excitation for Materials Characterization,* Ph.D. Dissertation, N. C. State University (2009) *http://www.lib.ncsu.edu/resolver/1840.16/5473*.
18. S. Asher, C. Johnson, and J. Murtaugh, "Development of a new UV resonance Raman spectrometer for the 217-400 nm spectral region," Rev. Sci. Instrum. **54**(12), 1657–1662 (1983).
19. S. Asher, *Coal Liquefaction Process Streams Characterization and Evaluation UV Resonance Raman Studies of Coal Liquid Residuals. DOE/PC/89883–67 (DE93009669)* DOE (1993).
20. American Petroleum Institute Research Project 44, *Selected Ultraviolet Spectral Data* **2** (1945–1984), Thermodynamics Research Center, Department of Chemical Engineering, Texas A & M University *http://catalog.lib.ncsu.edu/record/NCSU623743*.
21. J. M. Dixon, M. Taniguchi, and J. S. Lindsey, "PhotochemCAD 2: A refined program with accompanying spectral databases for photochemical calculations," Photochem. Photobiol. **81**, 212–213 (2005) *http://omlc.ogi.edu/spectra/PhotochemCAD/html/042.html* (benzene) http://omlc.ogi.edu/spectra/PhotochemCAD/html/090.html (toluene).
22. T. Etzkorn, B. Klotz, S. Sørensen, I. V. Patroescu, I. Barnes, K. H. Becker, and U. Platt, "Gas-phase absorption cross sections of 24 monocyclic aromatic hydrocarbons in the UV and IR spectral ranges," Atmos. Environ. **33**(4), 525–540 (1999) (MPI-Mainz-UV-VIS Spectral Atlas of Gaseous Molecules http://www.satellite.mpic.de/spectral_atlas.org).
23. K. G. Spears and S. A. Rice, "Study of the lifetimes of individual vibronic states of the isolated benzene molecule," J. Chem. Phys. **55**(12), 5561–5581 (1971).
24. J. H. Callomon, T. M. Dunn, and I. M. Mills, ""Rotational analysis of the 2600 Å absorption of benzene," Philos. Trans. R. Soc. London, Ser. A **259**(1104), 499–532 (1966).
25. E. B. Wilson, "The normal modes and frequencies of vibration of the regular plane hexagon model of the benzene molecule," Phys. Rev. **45**(10), 706–714 (1934).
26. T. C. Strekas, D. H. Adams, A. Packer, and T. G. Spiro, "Absorption corrections and concentration optimization for absorbing samples in resonance Raman spectroscopy," Appl. Spectrosc. **28**(4), 324–327 (1974).
27. H. Inaba, "Chapter 5: Detection of atoms and molecules by Raman scattering and resonance fluorescence," in *Laser Monitoring of the Atmosphere*, E. D. Hinkley, ed. Springer-Verlag, (1976).
28. P. G. Harmon and S. A. Asher, "Environmental dependence of preresonance Raman crosssection dispersions: Benzene vaporphase excitation profiles," J. Chem. Phys. **93**(5), 3094 (1990).
29. A. H. Willitsford, Johns Hopkins University - Applied Physics Lab, Laurel, MD 20709, and C. T. Chadwick, S. Kurtz, H. D. Hallen, C. R. Philbrick, are preparing a manuscript to be called "Resonance enhanced Raman scattering of the υ_9 and υ_{10} b_{2u} vibrational modes in the $^1B_{2u}$ absorption band."
30. D. R. Falcone, D. C. Douglass, and D. W. McCall, "Self-diffusion in benzene," J. Phys. Chem. **71**(8), 2754–2755 (1967).

1. Introduction

Many studies have documented resonance enhancements of Raman signals in benzene [1–6]. However, these studies were performed in the *pre*-resonance regime, which use excitation energies close to but not matching the absorption maxima. Here, we report first results from *on-peak*-resonance measurements (gains >500X), using fine tuning of the excitation wavelength to examine the resonance Raman scatter in the context of the absorption features present at and near the resonances. This study demonstrates an unexpected and interesting phenomenon: that the maxima in the resonance Raman enhancements actually occur when the excitation is positioned at wavelengths corresponding to the *vapor-phase* absorption maxima in samples of *liquid* benzene and *liquid* toluene. Specifically, the resonance enhanced Raman spectra in the $^1B_{2u}$ mode of the forbidden benzene electronic transition band, ~230-270 nm, has been investigated. We propose an explanation for this phenomenon based upon coherence

#196491 - $15.00 USD Received 27 Aug 2013; revised 6 Oct 2013; accepted 9 Oct 2013; published 24 Oct 2013

due to driving the resonance with photon energy matching a forbidden transition. We employ methods to calculate the resonance enhancement similar to the approach used by others [7,8].

The observation that resonance Raman, when excited on a forbidden transition, has the higher gain and narrower line width associated with a vapor phase absorption feature, while remaining in the liquid phase, has important implications stemming from the resultant large resonance gain values and therefore a sensitivity that is even higher than expected. This permits analysis of trace components even in a liquid state system, with particularly high impact on biological systems since many biological molecules are known to become rigid when desiccated. It also provides a scheme for remote detection of trace species [9–12], and enables nano-spectroscopic imaging [13,14] as a routine analysis.

2. Experimental approach

An Optical Parametric Oscillator (U-Oplaz) system produces a continuously tunable signal beam output in the wavelength range from 420 to 710 nm when pumped by the third harmonic of a Nd:YAG laser (Spectra Physics) [15–17]. Frequency doubling the OPO output with a β-BBO crystal generates the excitation source for this experiment, with an ultraviolet tuning range from ~210 nm to 355 nm. The OPO cavity uses a type-1 BBO crystal to generate a tunable signal with a wavelength dependent bandwidth of approximately 40 cm^{-1} at 260 nm. The OPO average power output is ~1 mW in the ultraviolet (depending on wavelength) with a 7-ns pulse length and a 10-Hz pulse repetition rate. In order to avoid saturation effects, the peak laser power densities are kept below 1 mW/cm^2, corresponding to the useful upper limit described previously [18,19]; the laser is not focused on the sample. The laser beam diameter of 0.8 cm typically provides a peak irradiance of ~0.4 mW/cm^2 for the measurements described in this paper. The Teflon sample cell at 45° to the incident beam uses sapphire windows mounted in a 90° scattering geometry, see Fig. 1. The laser light enters and scattered light exits through a window at the bottom of the sample cell, precluding any volume of vapor phase sample in the beam path. The scattered light is collected with a lens system and focused onto the slits of a Jobin Yvon Spex Triplemate 1877 spectrometer with a 2400 gr/mm grating blazed at 250 nm. Slit widths of 4.0 mm, 2.0 mm, and 250 μm are used for the input, filter, and main slits of the spectrometer, respectively. The spectrometer output is imaged onto an Andor Ixon (model: DU 897) back illuminated UV enhanced EM-CCD (Electron Multiplying-CCD) detector. Integration times of one to two minutes are typically used to achieve well defined Raman signatures with typical signal-to-noise ratios between 5 and 15.

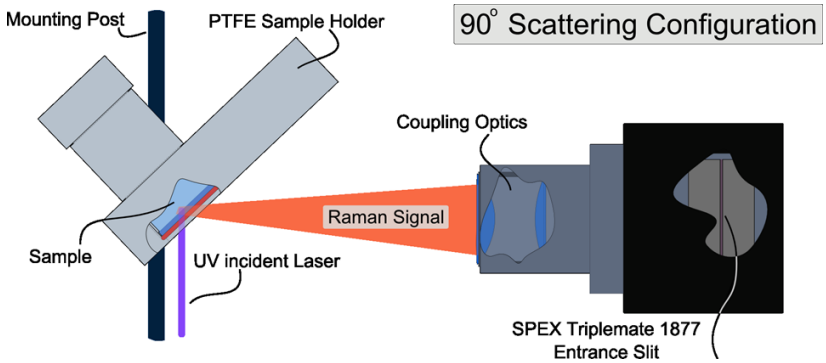

Fig. 1. Optical arrangement for the resonance Raman experiments.

3. Results

The benzene gas phase ($^1B_{2u} \rightarrow A_{1g}$) absorption band between 230 nm and 270 nm, shown in Fig. 2, contains several very narrow prominent absorption peaks with the larger peaks occurring near 253 nm and 259 nm [20–22]. The absorption feature at 259 nm was chosen for

#196491 - $15.00 USD Received 27 Aug 2013; revised 6 Oct 2013; accepted 9 Oct 2013; published 24 Oct 2013

detailed examination of resonance Raman scattering using narrow-width ultraviolet excitation because it experiences less self-absorption of the Raman scatter signals within the benzene. The periodic structure of the benzene vapor absorption exhibits maxima separated by a constant step on the order of 923 cm^{-1}, which corresponds to the energy of a strong resonance peak in the Raman spectra due to the ν_2 symmetrical ring-stretch mode of the excited state. When the Raman scattering excitation wavelength is 253 nm, the resonance Raman scattering peak occurs near 259 nm, where it is strongly self-absorbed according to the liquid absorption spectra. Excitation at 259 nm results in less self-absorption of the scattered ν_2 (993 cm^{-1}) ring-stretch mode at 265.8 nm, where the absorption in benzene is more than an order of magnitude smaller.

Graphs in Fig. 3 show the resonance enhanced Raman spectra of benzene for several excitation wavelengths near 259 nm. Each spectrum has been processed to remove background, normalized to remove the inherent Raman ν^4 dependence, and corrected for changes in laser power as a function of tuning wavelength. The particularly interesting result is that the maximum of the resonance enhancement occurs at the vapor-phase absorption peaks; even though the measurements are made in liquid benzene. The very large change in the maximum intensity, as the excitation wavelength is shifted by 0.25 nm steps, indicates that the resonance peak is likely even narrower, and the measured features are limited by the width of the excitation laser rather than the molecular properties. Thus, the actual resonance gain is expected to be larger if measured with a narrower-line laser and finer steps in excitation wavelength. Perhaps the most convincing evidence of this point is that the resonance Raman gain, as a function of increasing wavelength, begins low, rises, decreases, then again increases at the longest wavelength measured in this region, as does the vapor phase absorption, see Fig. 4. It is unlikely this could be explained by anything other than an interaction within the individual molecules and occurring on a short time scale [23,24]. For this to be the case, the Raman timescale must be short enough that the process involving an individual molecule is completed before energy can be exchanged with its neighbors in the liquid; therefore, the scattered signal responds as an isolated molecule (as in the vapor).

Figure 3 shows the relative intensity for the ν_2 (993 cm^{-1}, ring breathing) vibrational mode, along with a feature that could be identified as first overtone of the ν_{18} (2×608 cm^{-1}) vibrational mode (Herzberg ν_{18} is equivalent to Wilson ν_6 [25]), but which is actually the stiffened (strengthened) ν_{10} (1150 cm^{-1}) vibrational mode (Herzberg ν_{10} is equivalent to Wilson ν_{15}) [26]. Stiffening is observed as the excitation wavelength moves closer to the vapor-phase absorption peak and the excited state is probed. A resonance Raman excitation profile is constructed by integrating the area under each of the υ_2 and υ_{10} vibrational modes shown in Fig. 3. Those areas are plotted in Fig. 4 to illustrate the correlation between the relative intensities of the mode enhancements and the vapor-phase absorption features. As is evident in Fig. 4, the resonance of the Raman lines follows the vapor absorption rather than the liquid absorption, even when the sample is in the liquid state.

We have observed the same phenomenon in other species; for example, Fig. 5 shows the absorption corrected resonance Raman signal for liquid toluene, when scanning the excitation wavelength through its vapor-phase absorption peaks. A strong correlation is observed between the vapor phase absorption spectrum and the strength of the Raman scattered signal, similar to the observations in our benzene measurements. Again, we suggest that the forbidden nature of the absorption, where the Raman excitation is resonant, forces the timescale of the process to be short compared to the interaction time with the molecule's neighbors, so a coherent, single molecule (i.e., vapor) response is observed.

#196491 - $15.00 USD Received 27 Aug 2013; revised 6 Oct 2013; accepted 9 Oct 2013; published 24 Oct 2013

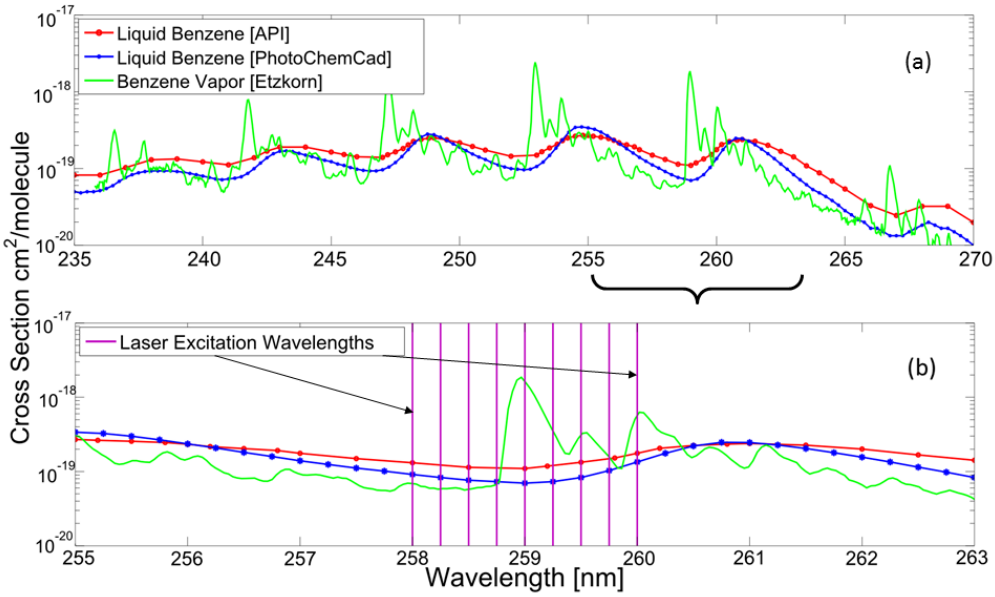

Fig. 2. Benzene liquid and vapor absorption spectra; (a) liquid spectra from API [20] and PhotoChemCad [21] are compared with benzene vapor absorption measured by Etzkorn [22] in the $^1B_{2u}$ band, (b) expanded plot showing locations of the laser excitation wavelengths used in Fig. 3.

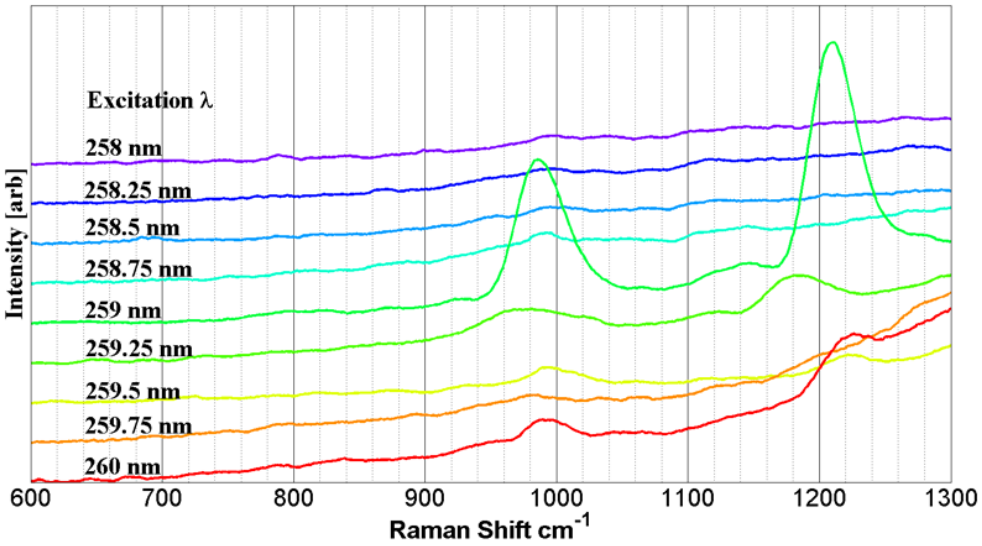

Fig. 3. Benzene resonance Raman spectra are plotted for several excitation wavelengths (each spectrum is offset) as the wavelength is stepped through a vapor absorption maximum.

#196491 - $15.00 USD Received 27 Aug 2013; revised 6 Oct 2013; accepted 9 Oct 2013; published 24 Oct 2013

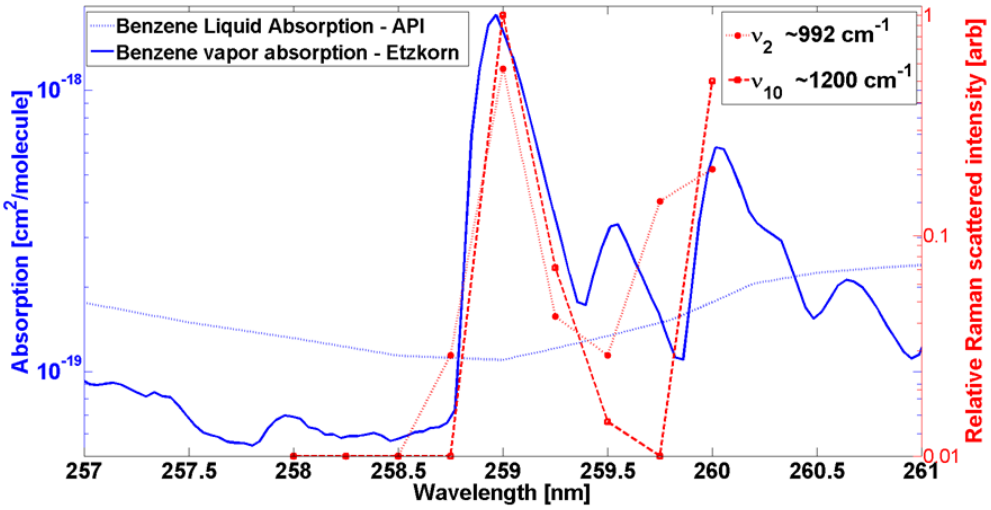

Fig. 4. Resonance Raman excitation profile for ν_2 (—•—) and ν_{10} (—•—) vibrational modes of benzene (right vertical axis). The absorption of benzene in the vapor (——) and liquid (- - -) phase are shown (left vertical axis). The experimental data clearly follow vapor absorption rather than that of the liquid.

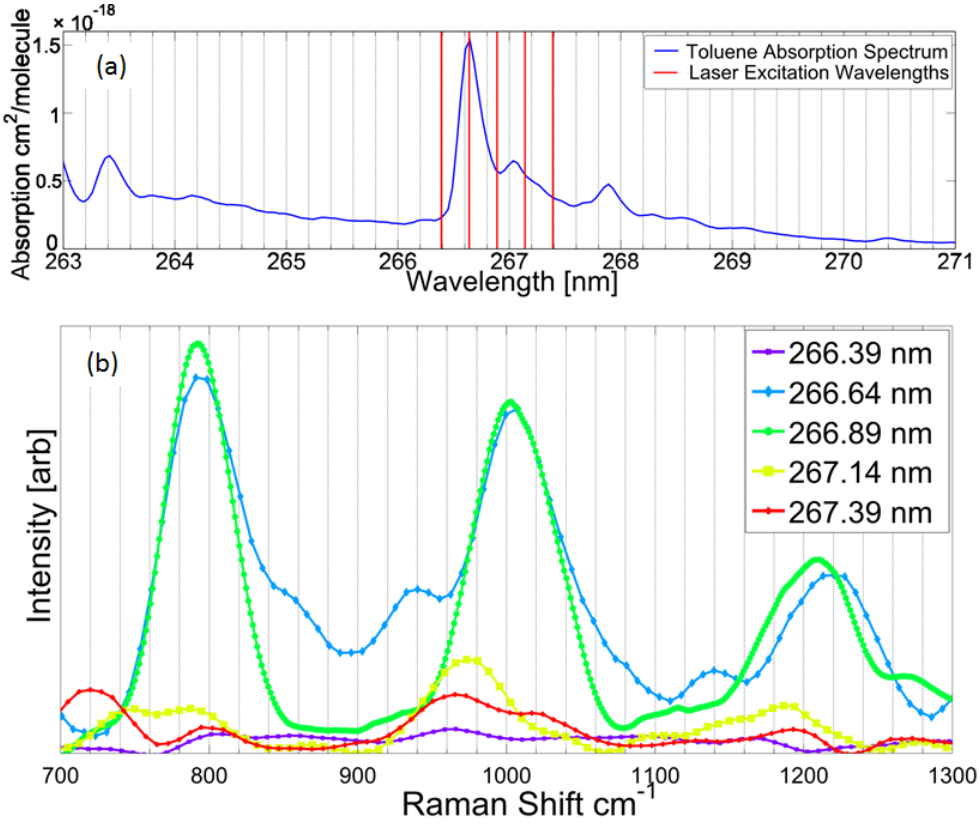

Fig. 5. Resonance Raman measurements of liquid toluene show correlation with the vapor-phase absorption features; (a) optical absorption of liquid toluene [22], (b) toluene resonance Raman spectra in this 1 nm wide excitation range.

#196491 - $15.00 USD Received 27 Aug 2013; revised 6 Oct 2013; accepted 9 Oct 2013; published 24 Oct 2013

We now discuss why the molecular time scale is short; this fact is more clearly seen when the excitation energy is not exactly at resonance. In Raman spectroscopy, a virtual interaction with the sample is limited by the Heisenberg uncertainty relation $\Delta t \geq h/\Delta E$. Here, ΔE is the energy difference between the nearest real state and the virtual state. The fact that this time is short is why Raman scattering is often termed an instantaneous process [27]. This Raman scatter time must be compared to the times for energy exchange with the surroundings. In other words, the time for the Raman process must be compared to the time for energy exchange with the neighboring molecules in a liquid or solid. If the interaction time is short enough, the dielectric function (defined in frequency, i.e., energy), would not apply. For purposes of this argument, the primary difference between the Raman process and the absorption process is the time scale of the interaction. The photons involved in absorption interact with the sample for as long as is required, thus, the dielectric function is a good indicator for the response. The short non-resonant Raman interaction need not follow the absorption curve, which can be calculated from the dielectric function. The important work of Harmon and Asher [28] gives further evidence that the short Raman time is important. They studied pre-resonance Raman enhancement in liquid and vapor phase benzene, in addition to other compounds, and found that the enhancement does not depend upon the phase of the material, in contradiction to the expectation that the enhancement should increase in the liquid state due to the increased local field strength created by the dielectric environment produced by the neighbors. If the dielectric screening is incomplete when the Raman process completes, then the enhancement would be similar to the vapor phase enhancement, as they observed. This underscores the ubiquitous importance of the Raman time in understanding the resonance Raman phenomenon.

Resonance Raman is usually considered a slow process, since the real intermediate state removes the Heisenberg constraint. However, the interaction time is still limited when the excitation is at a forbidden transition, one that requires a simultaneous phonon interaction. Since the $^1B_{2u}$ mode of benzene is a forbidden electronic transition, the resonance Raman from it requires a particular non-equilibrium position of the nucleus in conjunction with the Raman generation [7]. This requires a condition of resonance within the molecule itself, and is likely why the molecular resonance energy, rather than that of the liquid system, is required to describe the resonance Raman process. The resonance condition does not last long enough for the molecule to sense its surroundings. Korenowski et al. state [7] that "this contribution quite likely requires resonance conditions to be conspicuous because it requires a nuclear coordinate dependence of the electronic transition moment." Additionally Korenowski et. al. continue, stating that "in fact, all but one scattered fundamental are found to derive their intensity from states in the deep ultraviolet, not the $^1B_{2u}$. As such, the only fundamentals that will be resonant in such forbidden transition resonances will be totally symmetric." We experimentally observe that the only fundamental modes that are enhanced are symmetric: the symmetric ring-breathing mode υ_2 (992 cm^{-1}) fundamental, as well as the symmetric Kekule modes of υ_9 and υ_{10}. In addition, combinations and overtones are also observed to be resonantly enhanced [29].

An interesting observation in the work of Harmon and Asher [28] is that the symmetric ring-breathing mode υ_2 (992 cm^{-1}) pre-resonance enhancement data are fit very well when taking into account only resonances with modes to the blue side of the $^1B_{2u}$ mode of benzene. This means that the mode that we study here is not significantly involved away from resonance. Indeed, we see a dramatic decrease in the enhancement away from the very narrow resonance, Fig. 4. Apparently, the additional requirement for the intramolecular resonance significantly decreases the width of the resonance phenomenon such that it does not contribute to the pre-resonance above 280 nm, in the region studied by these researchers. Their observation is also consistent with our explanation for the phenomenon.

The strong response of the resonance excitation at vapor-phase absorption lines, rather than the liquid, leads to the question about whether some vaporous benzene might be present.

#196491 - $15.00 USD Received 27 Aug 2013; revised 6 Oct 2013; accepted 9 Oct 2013; published 24 Oct 2013

Note that we measure at the bottom of the liquid sample, through a window, so there is no surface vapor. If the liquid phase material (most of the material) contributed any resonant signal, the strongest response should be a broad maximum around 261 nm. We do not detect any Raman scattering at that wavelength, which suggests the surprising result that the liquid resonance is not important. There is some evidence that a vapor phase is eventually present in the sample, for reasons discussed elsewhere [17]. We have observed indications: light emission and audible popping, that a bubble is eventually formed (only) when the excitation energy is tuned precisely to the vapor resonance. This cannot describe the Raman resonance since typical bubble formation times (hundreds of nanoseconds to several microseconds) are orders of magnitude longer than the few nanosecond excitation pulse length, while the 0.1 seconds between pulses is very long compared to typical small bubble lifetimes. The molecules simply cannot respond to the energy input fast enough to attain vapor densities in nanoseconds. One might presume that a newly formed collection of excited molecules could become sufficiently disordered by the absorbed energy to exhibit vapor-like properties (lack of correlation and solvation with neighbors) while maintaining near liquid densities, but the excitation of a benzene molecule to a vapor-like state followed by a measurement before it relaxes is a nonlinear phenomenon, and we do not see evidence of a nonlinear dependence on excitation power. Further, if the signal is really due to a small subset of the molecules, then the enhancement would need to be much larger. In fact, if half of the photons were absorbed in the sample with 100% quantum efficiency, ~0.005% of the molecules would be excited, and the cross section for Raman scattering from these molecules, and not others, would need to be very large to explain the data. The fact that no resonance gain peak is found near the liquid absorption is unexpected, since there would be a much larger number of liquid-like benzene molecules present.

Finally, we address the question of possible sample damage. Due to the low fluence of our unfocussed beam, and due to the diffusion from the thin absorption layer [30], the impact of energy dissipation on our results should not be measurable. A simple calculation of the number of photons in the scattering volume implies that less than 0.01% of the benzene molecules would be damaged, assuming 100% quantum efficiency for damage. Liquid benzene has a self-diffusion coefficient of ~2.27 x 10^{-9} m^2/s [30], and the diffusion length (given the time between pulses) would be approximately 15 μm. The effective scattering volume is only a few microns thick at the resonant excitation wavelength, so multiple complete changes of the molecules in the scattering volume are expected before the next pulse.

4. Resonance gain

The magnitude of the resonance enhanced Raman scattering gain is not simply the ratio of peak areas. The benzene strongly absorbs both the excitation radiation and Raman scattered wavelengths in the ultraviolet region. We correct for the effect of absorption by estimating the number of molecules in a manner similar to the method used by Strekas et al. [25]. The resonance gain is considered to be a separate gain from the inherent frequency dependent increase in Raman scattering cross-section, and the data have been pre-corrected to account for this power dependence (ν^4). Additionally, the data have been corrected for differences in quantum efficiency of the camera detector, as well as throughput efficiency of the spectrometer. Therefore, the overall resonance gain for the ν_2 vibration can be calculated by comparing the relative intensities, and the relative number of scatters, in the cases of the resonance and off-resonance Raman scattered signals.

The relative intensity of the Raman scattered mode is determined by the area under the curve of the Raman scattered signal using a best-fit Gaussian curve. The number of scattering molecules is determined by estimating the scattering volume and density of benzene. In our case, the ν_2 vibration is chosen for the parameters used in calculating the figure of merit for the resonance enhancement, as this feature is clearly observed in both the resonant and off-

#196491 - $15.00 USD Received 27 Aug 2013; revised 6 Oct 2013; accepted 9 Oct 2013; published 24 Oct 2013

resonant Raman spectra. In particular, the relative intensity of the Raman scattered signals of the ν_2 vibrational mode were fit with Gaussian curves as shown in Fig. 6. These Gaussian fits were used to determine the area under the curve for the resonant (259 nm) and non-resonant (430 nm) excitations:

$$\text{Gaussian fit area ratio} = \frac{\text{area of 259 nm } \nu_2}{\text{area of 430 nm } \nu_2} = \frac{1.56}{2.11} = 0.74 \pm 10\%$$

The primary factor in determining the resonance gain is the number of scattering molecules, and is based on the minimum of the volume illuminated by the excitation source (UV) or the volume from which signal is collected (visible). In both cases, the density of the liquid state is used to calculate number of molecules, since any bubble formation will only take place after the laser pulse has passed and Raman signals have been emitted as noted above. We assume Beer's law is valid in the UV, and calculate the absorption length. As the laser excitation wavelength is tuned through the absorption maximum, the laser effective sampling depth drastically falls due to the rapid extinction from the absorption. Figure 7 illustrates the paths where self-absorption of the Raman scattered component and the attenuation of the excitation beam occur.

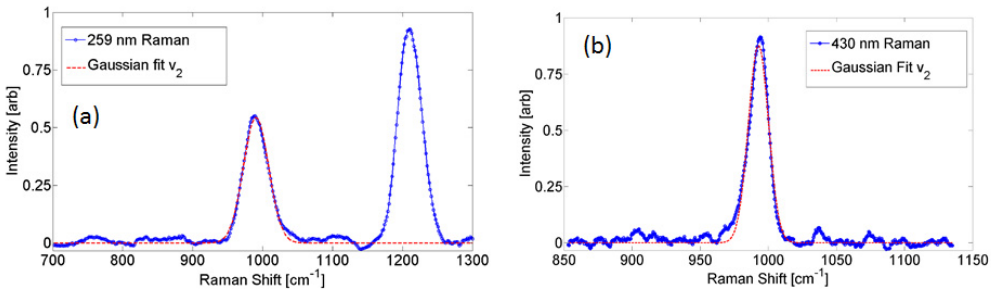

Fig. 6. Gaussian curve fits to Raman signals of the ν_2 state; (a) 259 nm excitation Raman spectra, (b) Raman spectrum for 430 nm excitation.

The calculation can be separated into two steps; first, the absorption along the excitation laser path is calculated, and then the absorption on the exit path for the Raman scattered wavelength is calculated. Figure 7 shows the path lengths used to calculate the absorption and effective volume of scattering. The loss on the entry path can be described as,

$$I/I_0 = \exp\left(-d_{in}\alpha_{excitation}\right), \text{where } d_{in} = \boldsymbol{x}/\cos(\theta)$$

where $\alpha_{excitation}$ is the absorption coefficient at the excitation wavelength. The loss on the exit path (Raman scatter) is,

$$I/I_0 = \exp\left(-d_{out}\alpha_{Raman}\right), \text{where } d_{out} = \boldsymbol{x}/\sin(\theta),$$

where α_{Raman} is the absorption coefficient at the Raman scattered wavelength. Thus, the total loss over the distance $\boldsymbol{X}$ (deepest penetration laser penetration depth) is averaged to find an effective sampling depth, from which all scattering would take place,

$$\text{effective sampling depth} = \int_0^x \exp\left[-\alpha_{excitation}x'/\cos(\theta) - \alpha_{Raman}x'/\sin(\theta)\right]dx'. \qquad (1)$$

The absorption coefficients are the product of the cross section and the number density, 6.78×10^{21} molecules / cm^3 for the liquid.

#196491 - $15.00 USD Received 27 Aug 2013; revised 6 Oct 2013; accepted 9 Oct 2013; published 24 Oct 2013

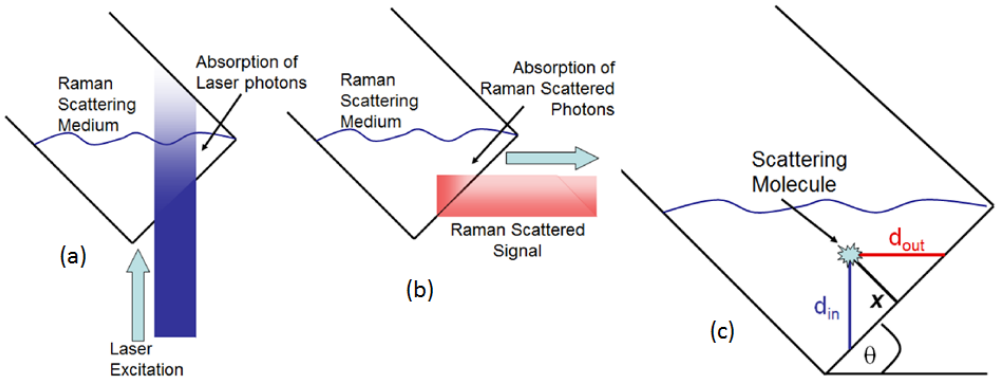

Fig. 7. Diagram shows; (a) a portion of the laser excitation absorption and self-absorption, (b) the Raman scattered signal, and (c) the absorption loss and scatter paths calculated using the distance ***X*** from the laser entry point. The distance d_{in} is the path length of the excitation wavelength, d_{out} is the path length of the Raman shifted wavelengths, and the sample window is held at $\theta = 45°$.

The effective sampling depth, for resonant excitation near 259 nm in benzene, calculated using Eq. (1), is approximately 7 μm, when applying the liquid phase absorption cross-section of 1.16×10^{-19} cm^2/molecule at 259 nm and 3.32×10^{-20} cm^2/molecule at the Raman shifted 265.85 nm and using the liquid density [22]. In the case of non-resonant excitation at the visible wavelengths, the depth of sampling is approximately equal to the slit height (20 mm) divided by the magnification (5X), yielding 4 mm. The error in the calculated gain is dominated by the estimation of the number of scattering molecules in our scattering volume, and is about ± 10%. The ratio of the active volume for the visible wavelengths to the volume of the resonance Raman scattering at ultraviolet wavelengths is ~600. The overall gain for the ν_2 vibrational mode in benzene can be found by multiplying the ratio of Raman scattered intensities (0.74) and the ratio of the effective scattering volumes (~600) yielding a resonant enhancement of 450 ± 10%.

The resonant enhancement of the ν_2 mode of benzene was also examined at the largest vapor-phase absorption peaks near 253 and 247.2 nm. Figure 8 shows the resonance enhancement near the vapor peak absorption for these two wavelengths; note that the wavelength of the excitation peak is pulled toward shorter wavelength (stiffening) as the narrow energy state is approached. The resonant excitation depth near 253 nm in benzene, calculated using Eq. (1), is approximately 4.8 μm when applying the liquid phase absorption cross-section of 1.49×10^{-19} cm^2/molecule at 253 nm and 1.33×10^{-19} cm^2/molecule at the Raman shifted 259.57 nm and using the liquid density. The resonant excitation near 247.2 nm in benzene, calculated using Eq. (1), is approximately 5 μm when applying the liquid phase absorption cross-section of 1.39×10^{-19} cm^2/molecule at 247.2 nm and 1.84×10^{-21} cm^2/molecule at the Raman shifted 253.46 nm and using the liquid density [22]. The Raman scatter spectra obtained for several steps with a bandwidth of ± 0.5 nm are shown in Fig. 8 for these excitation wavelengths. The ratio of Raman scattered intensities and sampling depths were calculated for these cases as well, yielding gain factors of 600 ± 10% at 253 nm, and 600 ± 10% at 247.2 nm.

Figure 9 shows the spectra measured between 252 and 272 nm when the excitation wavelength was changed from 259 to 253 nm, then to 247.2 nm. The magnitude of the fluorescence interference in the Raman spectra is found to be markedly less at short wavelengths. The fluorescence background increases at wavelengths greater than ~267 nm; however, using deeper UV excitation allows retrieval of Raman signals without interference from the strong fluorescence background signals.

#196491 - $15.00 USD Received 27 Aug 2013; revised 6 Oct 2013; accepted 9 Oct 2013; published 24 Oct 2013

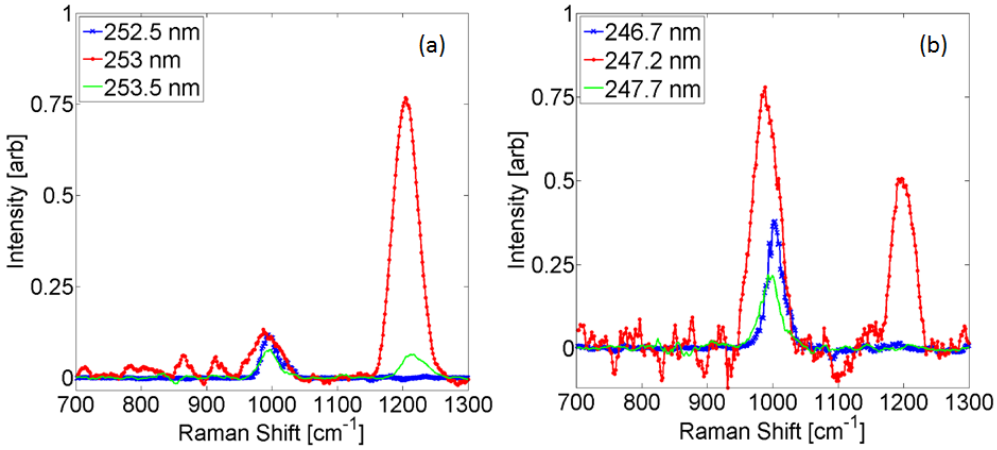

Fig. 8. (a) Resonance enhanced Raman scatter around the 253 nm peak absorption wavelength. (b) Resonance enhanced Raman scatter around the 247.2 nm peak absorption wavelength in benzene.

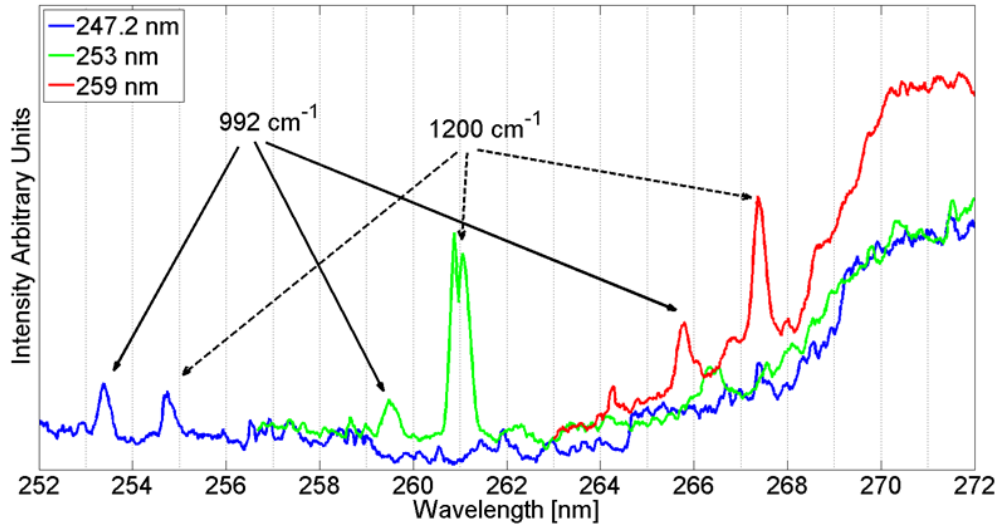

Fig. 9. Raman spectra on a wavelength scale showing fluorescence background of benzene liquid increase as the excitation steps toward longer wavelengths. The wavelength range of fluorescence emission is rather independent of the excitation wavelength, while the Raman signals (notably narrow peaks at 992 cm^{-1} and 1200 cm^{-1}) shift with the excitation.

5. Conclusion

An investigation of the resonant enhanced Raman spectrum of liquid benzene using a ~0.25 nm bandwidth excitation wavelength is reported. Measurements were made while tuning through the regions of the ultraviolet absorption features between 230 and 270 nm. Resonance Raman gain factors of 450, 600, and 600 are found corresponding to excitation wavelengths of 259, 253, and 247.2 nm, respectively. The major enhancements in the liquid-sample Raman scattered spectrum coincide with the wavelengths of the vapor-phase absorption peak maxima of the $^1B_{2u}$ band of benzene. This effect is explained by a short Raman time enforced by the *intra molecular resonance* condition required to allow resonance Raman emission on this forbidden electronic transition. In addition, the same effects are observed in liquid toluene when scanning the excitation wavelength through the vapor phase absorption.

#196491 - $15.00 USD Received 27 Aug 2013; revised 6 Oct 2013; accepted 9 Oct 2013; published 24 Oct 2013

The advantage of enhancement from vapor phase lines rather than liquid phase lines stems from the much narrower line widths of the vapor phase. The narrow line means a much larger enhancement and much larger signal to noise ratio in an experiment. This work identifies a means by which to choose excitation wavelengths to take advantage of this phenomenon in many types of materials: a forbidden transition must be identified; its excitation should influence the molecule so that a totally symmetric vibration mode of interest will be enhanced. In the case of benzene and toluene, a forbidden transition disrupts bonding around the aromatic ring, so the ring-stretch mode is strongly impacted and resonates. The choice in general will depend upon the molecule and sites of interest.

Acknowledgments

We thank Michigan Aerospace Corporation for the loan of their Andor (EMCCD) camera. We also would like to thank Dr. Arthur Sedlacek of Brookhaven National Labs and Dr. Sanford Asher of the University of Pittsburgh for their helpful discussions. The laser source is part of an instrument developed under NSF grant DMR-9975543.

#196491 - $15.00 USD Received 27 Aug 2013; revised 6 Oct 2013; accepted 9 Oct 2013; published 24 Oct 2013